Correlation approach for testing and simulation of MetOp-SG Ice Cloud Imager full structure, 183 to 664 GHz.

David Marote[1], Marc Bergadà[1], Gloria Amazares[2], Pedro Robustillo[3], Jakob Rosenkrantz de Lasson[4], Cecilia Cappellin[4], Ulf Klein[5]

[1]Airbus Defence and Space SAU (ASE), Avenida de Aragon 404, 28022 Madrid, Spain, David.Marote@airbus.com
[2] HI Iberia, Madrid, Spain.
[3]Airbus Defence and Space D-88039 Friedrichshafen, Germany, Pedro.Robustillo@airbus.com
[4]TICRA, Landemærket 29, DK-1119 Copenhagen, Denmark, jrdl@ticra.com
[5]European Space Agency (ESA/ESTEC), Keplerlaan 1, Noordwijk, The Netherlands, Ulf.Klein@esa.int

***Abstract* - This paper presents the latest status of the full-wave simulation of MetOp-SG Ice Cloud Imager (ICI) and the methodology proposed to correlate both simulation and antenna pattern testing in two cases, namely for the main beam and the full 4π. In addition, the main features of the compact range belonging to the selected test facilities are presented.**

***Key words*- MoM/MLFMM, Multi-GTD, PEC, correlation, sunshield, mm-wave, full wave.**

I. INTRODUCTION

ICI is a conical scanning microwave radiometer that will be mounted on the MetOp-SG Satellite B. The purpose of ICI is to monitor cloud ice particles by means of brightness temperature retrievals. More details on ICI are included in [1]. Table 1 contains the description of each ICI channel.

Channel name	Frequency (GHz)	Simplified Utilisation
ICI-1	183.31±7.0	Water vapour profile and snowfall
ICI-2	183.31±3.4	
ICI-3	183.31±2.0	
ICI-4 (dual-pol)	243.2±2.5	Quasi-window, cloud ice retrieval, cirrus clouds
ICI-5	325.15±9.5	Cloud ice effective radius
ICI-6	325.15±3.5	
ICI-7	325.15±1.5	
ICI-8	448±7.2	Cloud ice water path and cirrus
ICI-9	448±3.0	
ICI-10	448±1.4	
ICI-11 (dual-pol)	664±4.2	Cirrus clouds, cloud ice water path

Table 1: ICI channel definition

These 13 double side-band channels operating between 183 and 664 GHz are achieved by means of a feed cluster of seven horns in a single offset-reflector configuration. Cold calibration is performed when the rotation scanning allows the feed cluster to intercept the so called cold-sky reflector. In order to guarantee stable thermal conditions, a conical Carbon Fibre Reinforced Polymer (CFRP) sunshield protects the antenna system and the electrical units from radiation and sun intrusion.

Since the operating frequencies are very high, the structure is electrically very large. As presented in [2], the electrical size of the problem invites for the use of high-frequency simulation techniques, such as Multi-Geometrical Theory of Diffraction (Multi-GTD). On the other hand, the fact that ICI is a semi-closed structure, with a quasi-resonant behaviour, implies that the use of a ray-based technique, such as Multi-GTD, requires the inclusion of an important number of interactions[1] between elements. Furthermore, Multi-GTD analysis is a labour intensive task that requires an exhaustive knowledge of any single task of the simulations.

After an overall review of Multi-GTD pros and cons, it seems that the most convenient modelling approach is the use of full-wave analysis techniques, such as Method of Moments (MoM), or any of its efficient implementations, such as the Multi-Level Fast Multipole Method (MLFMM), as implemented in GRASP [7]. In [3], TICRA describes the tasks for the upgrading of Planck telescope simulations, which was an important step to enhance MoM/MLFMM computations in GRASP.

Nevertheless, if we want to address the ICI solution from a purely full-wave analysis, we face that the memory requirements would be around 1.5 TB at 183 GHz to approximately 19 TB at 664 GHz [2], even with the very efficient computation methodology of GRASP.

[1] In [2], the maximum order of the Multi-GTD reflections and diffractions included in the computations was 5th, and it was shown that this was not sufficient to achieve the same accuracy as for MoM simulations.

In [4] Taboada *et al*. describe an approach for the MoM computation suitable for large supercomputer clusters.

In this report we introduce an alternative simulation approach to the one proposed in [2], using one of the GRASP modelling capabilities, the *Composite MoM/MLFMM* object.

The first part of this Introduction is related to electromagnetic (EM) simulations; nevertheless, EM simulations are just one half of the full picture. They are the means to ensure that the performance of the designed instrument (including surrounds) meets the requirements. The second, and not less important, part of the work is the antenna pattern test campaign. ASE has contracted Airbus DS Ottobrunn to perform this state-of-the-art task. An example of the experience of Airbus with high frequency challenges within ESA frame is described in [5], the Admirals test campaign. Along this test campaign, frequencies up to 503 GHz were tested within Airbus' Compensated Compact Range (CCR) facilities. Similar tasks were performed during the Planck telescope test campaign [6].

Following the presentation of the simulations and the test range, we introduce the antenna pattern performances. The Half Power Beam Width (HPBW) of the radiation pattern for the ICI main beam is almost constant with frequency, with a value of ~0.5º and a peak level around 51 dBi and (far) Sidelobes level > 60 dB below peak. This delta-like characteristic is a driving factor to do a proper correlation approach. On the one hand, we have to ensure that the simulations are sufficiently accurate on both the main beam and 4π patterns, and on the other hand the CCR quiet zone needs to ensure a high signal-to-noise level to guarantee sufficient accuracy to detect any significant manufacturing and/or alignment deviations.

In summary, we have to combine three main aspects:

- the ICI EM simulation,
- the radiation pattern characteristics
- and the CCR performances

The merging of the three points requires an adequate approach in order to be efficient with respect to the CPU and memory needs vs. required simulation accuracy on one side, and the CCR performances that can be achieved at ICI frequencies on the other.

The structure of the paper is as follows: Section II describes the considered simulation approach for Metop-SG ICI including the current status of simulations. We continue in Section III with the test range capabilities expected for ICI pattern characterisation. Section IV contains the correlation approach for the main beam and for the 4π patterns. Finally, Section V provides a summary of the work.

II. ICI GRASP MODELLING

A. *Introduction*

In this paper, we will focus on the MoM simulation with the objective of exploring the feasibility of using this technique for ICI full wave simulation. The simulated structure of ICI is depicted on Figure 1.

It includes the following elements:

Geometrical elements: Main reflector, rotating platform, sunshield an extension cylinder to the fixed platform, annular shield, central cylinder, fixed platform,

Electrical elements: ICI feed horn radiation pattern.

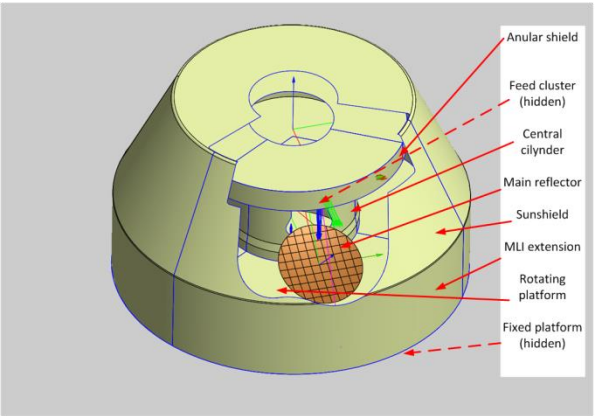

Figure 1: CAD model of ICI as used in GRASP.

B. *Modelling Approach*

After a detailed review of GRASP capabilities, we propose the use of the GRASP object *Composite MoM/MLFMM Scatterer* as the kernel to build the EM model. This element allows individualising the electrical properties and simulation accuracy of each geometrical object. Thus, it goes further than the widely known (for GRASP users) *Scatterer Cluster* object. The *Composite* element is adequate for the ICI purpose for three reasons:

1. It is devoted to MoM/MLFMM computation.
2. It permits to specify the conductivity properties of the material. This option is convenient for ICI purpose due to the fact that the major part of the internal structure is covered by bare

CFRP, whereas the main reflector is gold coated aluminium[2].

3. It allows changing the accuracy of the simulation. This feature is suitable due to the fact that by reducing the accuracy of the simulation, the memory requirements can be reduced significantly.

For a given accuracy requirement, for example a relative error of 0.001, the convergence speed of the simulations depends on the operating frequency and on the conductivity properties of the elements. The PEC case requires the higher number of algorithm iterations in comparison to a lossy conductor surface, because the lossy material helps to absorb part of the electromagnetic energy that bounces around inside the ICI sunshield.

Further details about MoM/MLFMM characteristics can be consulted in [2], [3] and [7].

C. Smart EM modelling

This sub-section contains the description of the proposed ICI full wave simulation way forward. Current in-house ASE computation capabilities are as specified in Table 2.

2x Intel(R) Xeon(R) CPU E5-2699 v4 @ 2.20GHz, 2197 Mhz, 22 proccesors
256 GB RAM
3.5 TB SSD memory

Table 2: CPU features for ICI simulations

For full-wave simulation purposes, we consider the central frequency of the lower ICI channel, 183.31 GHz. According to [2], the memory requirements for 183.31 GHz frequency is ~1.5 TB, using the MLFMM approach. After several iterations and trade-off studies, a total memory requirement of 0.5 TB can be handled thanks to the GRASP capability of allowing the sharing of memory among the RAM and the hard disk. The penalty of using a hard disk for the computation is the total computing time. In order to minimise this drawback, ASE uses a 3.5 TB SSD for the simulations.

Now that the memory restrictions are described, we proceed to the proposed solution to cope with the full-wave simulation.

The solution is based on the fact that the main beam radiation pattern is a pulse, 0.5 degrees of HPBW, and the total spill-over is in the range of 1%. We split the problem in two parts, related to so-called front and back volumes.

[2] For the current simulations we consider the reflector surface as a perfect electric conductor (PEC). The surfaces of the ICI structure (CFRP) are modelled including losses.

The front part contains an angular portion of ~120 degrees centred in the main reflector, as highlighted in blue in Figure 2. For this front part, we will require the normal accuracy.

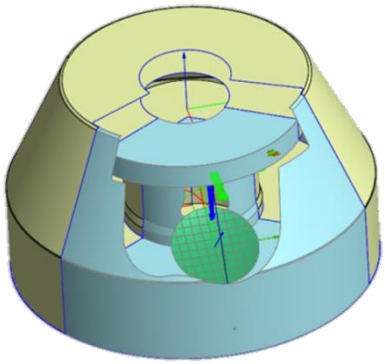

Figure 2: Front part (blue) of ICI, normal accuracy

The rear part contains the rest of the angular region, ~240 degrees, as indicated in blue in Figure 3. For this rear part, we require a reduced accuracy by, in the *Composite MoM/MLFMM Scatterer*, setting the accuracy to *Reduced*.

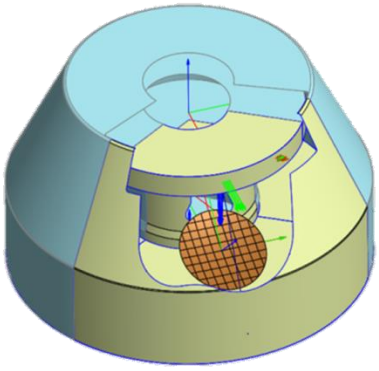

Figure 3: Rear part (blue) of ICI, reduced accuracy

Thanks to this option, the total memory requirement at the 183.31 GHz simulation is reduced from the initial estimation of ~1.5 TB, to approximately 0.5 TB. The benefit of this simulation strategy is that the whole ICI structure is simulated using a full-wave technique (MoM/MLFMM), and the effects from the quasi-enclosed cavity formed by the sunshield are thus handled rigorously.

Table 3 contains selected computing values extracted from the simulations. The CAD model is meshed

according to the frequency and accuracy requirements, providing the number of unknowns, and thus giving the total memory requirements.

Parameter	Value
Total unknowns	~33,000,000
Total memory	~ 500 GB

Table 3: Computing requirements, 183.31 GHz.

D. Radiation pattern examples

Figure 4 shows the ICI radiation pattern from the 4π simulation at 183.31 GHz. The tiny point, (centred and with a cross) with approximately 51 dBi at peak, is the main lobe. Figure 4 is very illustrative because of it reflects clearly the great difficulty which is to characterise correctly the 4π pattern, either by simulation or by test measurements. The full sphere pattern is composed by a very high level and narrow signal plus all the interactions of the almost-closed sunshield cavity and the scattering coming from the rotating and fixed platforms. The showed signal levels vary from peak, ~52 dBi, down to -35 dBi, i.e., ~90 dB of dynamic range.

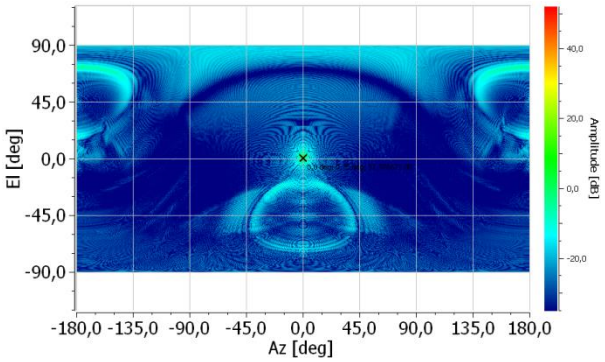

Figure 4: 4π pattern (Elevation [-90º:+90º] over Azimuth [-180º:180º])

Figures 5 and 6 display a zoom of the co- and cross-polar components (according to Ludwig's 3rd definition) around the main beam,.

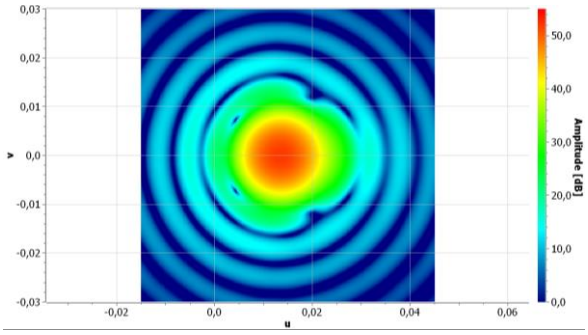

Figure 5: Main beam zoomed area. Co-polar component 183.31 GHz.

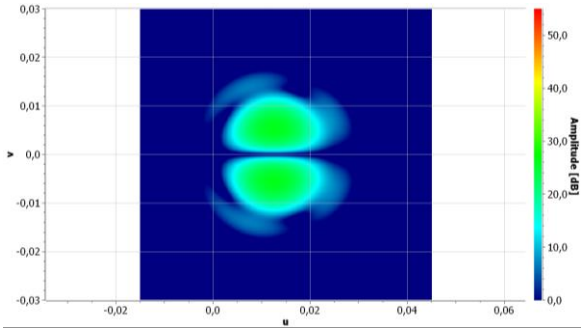

Figure 6: Main beam zoomed area. Cross-polar component 183.31 GHz.

Figures 7 and 8 show co-polar radiation pattern cut examples.

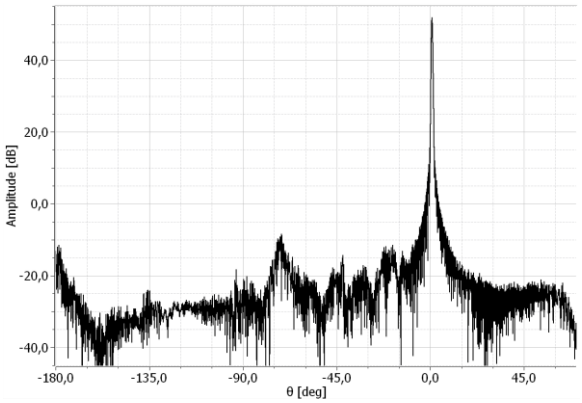

Figure 7: Co-polar radiation pattern, (ϕ= 0º, θ=[-180 :70º]), 183.31 GHz

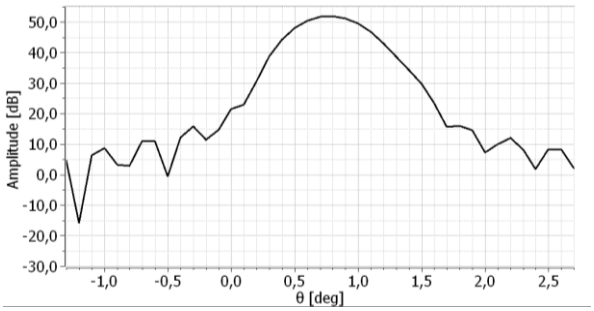

Figure 8: Co-polar radiation pattern (zoom), (ϕ=0º, θ=[-1.3 :2.7º]), 183.31 GHz

III. TEST FACILITIES DESCRIPTION

The selected test facility for the ICI test campaign, Airbus DS Ottobrunn, is an outstanding test centre with a vast experience in highly demanding test campaigns. Among all experience on telecom and Earth observation missions, where they are a reference centre in the space industry, the CCR 75/60 has participated in the ADMIRALS test characterisation. This study was

performed from 2000 to 2005, and a paper that summarizes this work is [5].
Extracted from this paper we have Table 4, which summarises the worst case Error budget of CCR 75/60 achieved for frequencies between 203 GHz and 503 GHz. This table is the starting point to have an idea of the potential test capabilities expected for ICI.

Error	Pattern Level [dB]	Error [dB] 203 GHz	Error [dB] 322 GHz	Error [dB] 503 GHz
Feed polarisation	- 30	**0.15**	**0.15**	**0.15**
Feed alignment	- 30	**0.00**	**0.00**	**0.00**
Feed mismatch	- 30	**0.00**	**0.00**	**0.00**
Reflector surface	- 30	**0.38**	**0.60**	**1.30**
Serrations and billboard co-pol.	- 30	**0.30**	**0.30**	**0.30**
Serrations and billboard x-pol.	- 30	**0.23**	**0.23**	**0.23**
Direct leakage suppression	- 30	**0.02**	**0.02**	**0.02**
Quiet zone taper on AUT	- 30	**0.00**	**0.00**	**0.00**
AUT positioning system	- 30	**0.05**	**0.07**	**0.10**
AUT mismatch	- 30	**0.00**	**0.00**	**0.00**
Receiver amplitude non-linearity	- 30	**0.30**	**0.30**	**0.30**
Receiver dynamic range	- 30	**0.07**	**0.07**	**0.07**
Multiple reflections	- 30	**0.15**	**0.15**	**0.15**
Room scattering	- 30	**0.15**	**0.19**	**0.25**
Leakage and crosstalk	- 30	**0.05**	**0.05**	**0.05**
Other errors	- 30	**0.05**	**0.05**	**0.05**
X-pol error	- 30	**0.90**	**0.90**	**0.90**
Resulting error co-polar (RSS):	- 30	**0.66**	**0.81**	**1.41**
Resulting error x-polar (RSS):	- 30	**1.10**	**1.19**	**1.64**
Resulting error co-polar (RSS):	- 40	**1.94**	**2.35**	**3.84**
Resulting error x-polar (RSS):	- 40	**3.08**	**3.31**	**4.38**

Table 4: Worst Case Error Budget for Pattern Measurements in CCR 75/60. Extracted from [5]

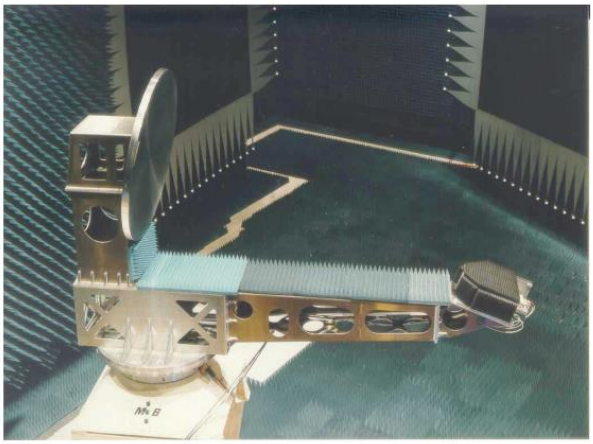

Figure 9: ADMIRALS RTO mounted on DUT Positioner of CCR 75/60. Courtesy of Airbus DS GmbH, Ottobrunn. Extracted from [5]

For the ICI test campaign, the set-up is adapted to ICI features according to RX linearity, antenna pattern gains and operating frequency.

In summary, the difficulty of the pattern characterisation relies not only on the simulation, but also in the radiation pattern test.

IV. CORRELATION APPROACH

After an overall review of the simulation and pattern characteristics, jointly leading to the expected performances in the test facilities, in this section we treat the proposed correlation of both measurements and simulations.

We distinguish two cases, the main beam radiation pattern and the 4π patterns.

Table 5 contains the absolute error level for a given noise floor of 70 dB below peak, reference noise level for this example.

Signal level. dB below peak	Error (dB)
-5	[+0.005, -0.005]
-10	[+0.009, -0.009]
-20	[+0.03, -0.03]
-30	[+0.09, -0.09]
-40	[+0.27, -0.28]
-50	[+0.83, -0.92]

Table 5: Error (dB) for a given signal-to-noise ratio. (Data referred to 70 dB below peak noise floor).

A. *Main Beam correlation*

As Figure 10 shows, once the CCR noise floor is determined, the main issue for this measurement is to detect accurately the main beam peak, and then to test the signals to a level about 40 dB below peak, which corresponds to an absolute level of ~10 dBi.

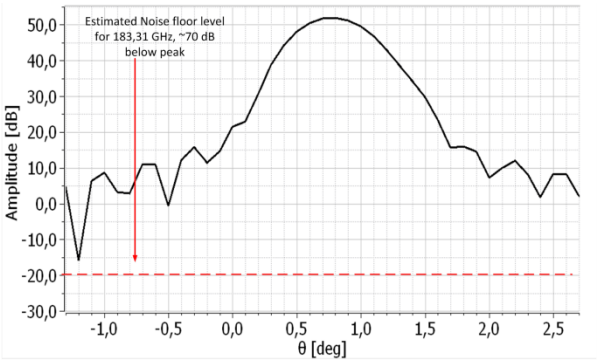

Figure 10: Main beam pattern cut (ϕ=0º, θ=[-1.3 :2.7º]) at 183.31 GHz and noise floor (dashed line)

For this main beam correlation, and for the higher frequency channels, up to 664 GHz, we propose to follow the same approach. The antenna pattern for this correlation can be the one obtained using only the feed horn radiation pattern plus the main reflector.

B. *4π correlation*

The 4π measurement serves to check that the predicted pattern behaviour and the tests are within expected levels and angular ranges. In this measurement, the main beam characterisation is less relevant than for the specific main beam radiation pattern. In fact, the angular step to be tested is 0.5 degrees, which corresponds to the beam HPBW, and therefore the main beam will be represented sparsely by only three to four sample points.

In addition, the expected CCR noise level will be between 70 to 80 dB below peak. The major part of the ICI signal level is lower or in the range of the noise floor level. Taking 70 dB as a worst case scenario at 183 GHz, the next task is to identify, in advance of the measurements, the relevant pattern features to serve as validation points. Figure 11 sketches this approach where the dashed line represents the noise floor level, and where circles enclose the pattern regions suitable to be checked.

We note that there are alternatives to increase the dynamic range of the CCR for the lower level signals based on the achievable linearity of the amplifiers.

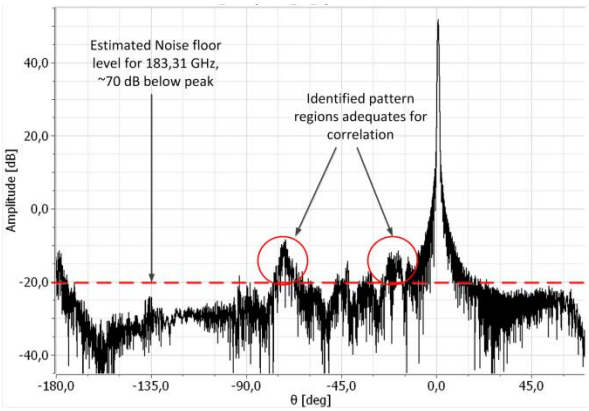

Figure 11: ICI co-polar pattern cut (ϕ= 0º, θ=[-180 :70º]) 183.31 GHz, with pre-identified areas for 4π correlation.

V. SUMMARY AND CONCLUSIONS

We have introduced the modelling and testing issues that a state-of-the-art high-frequency microwave instrument as ICI presents.

On the simulation side, a key problem is the total amount of memory vs. accuracy that it is needed for a full-wave characterisation. We consider that at least for the lower frequency (183.31 GHz) it is important to perform a full-wave simulation, as explained in the Introduction. The difference between ICI and other microwave radiometers is that the lower frequency is ~183 GHz, and the highest operating frequency is 670 GHz. Thus, although the ICI structure is approximately 1 m^3, the electrical size of the problem is relatively large and requires ~1 billion of unknowns at mm frequencies. The proposed simulation approach consists of splitting the problem in two parts, one for the front part with normal accuracy, and one for the rear part with reduced accuracy, which permits to compute accurately full-wave simulations at 183 GHz. Indeed, the simulation is performed including the two parts in the same simulation. For higher operating frequencies, 243 GHz and above, a combination of PO+PTD feed+main patterns and the knowledge gained from the 183.31 GHz full-wave pattern could be a potential solution. The use of Multi-GTD + PO+PTD is also an alternative [2].

Regarding the radiation pattern measurement and the correlation with the simulations, we envisage that the noise floor level of the CCR may not be sufficient as the far-lobes pattern level is more than 70 dB below peak, i.e., is in the range or lower than the CCR noise floor. For this reason, a strategy is proposed where the objective is to detect and check that the higher far sidelobes levels appear in both simulation and measurements.

VI. REFERENCES

[1] Marc Bergadà, Miguel Ángel Palacios, Massimo Labriola, David Marote, Ana Andrés, Raquel González, Jean-Claude Orlhac, Ulf Klein (2017). The Ice Cloud Imager: design status, predicted performance and verification. *ARSI 2017.*

[2] J. R. de Lasson, P. H. Nielsen, C. Cappellin, D. Marote, M. Bergada, R. Gonzalez, P. de Maagt. (2017). Full-Wave and Multi-GTD Analysis of the Ice Cloud Imager for MetOp-SG, *EuCAP 2017.*

[3] E. Jørgensen, P. H. Nielsen, O. Borries, and P. Meincke, (2015). Full-wave modelling of the Planck telescope, *36th ESA antenna workshop*

[4] J.M. Taboada, L. Landesa, F. Obelleiro, J.L. Rodríguez, M.G. Araújo, J.M. Bértolo (2010) MLFMA-FFT Parallel Algorithm for the solution of Large-Scale Problems in the Electromagnetics. *Progress in Electromagnetcs Research, Vol. 105, 15-30, 2010.*

[5] J. Hartmann, J. Habersack, H.-J. Steiner. (2007) Analysis and measurement of Reflector Antennas in the mm-wave Frequency Range. *2nd Internationl ITG Conference on Antennas*

[6] G. Forma, C. Nardini, H. Garcia, C. Bouvin, D. Allenic, D. Laibe, , S. Navasackd, D. Dubruel, J. Marti Canales, G. Crone, J. Tauber (2006) 30-70-100-320 GHz Radiation Measurements for the Radio Frequency Qualification Model of the Planck Satellite. *EuCAP 2006.*

[7] GRASP Software, TICRA, Copenhagen, Denmark, www.ticra.com